JOURNAL OF THE GEOLOGICAL SOCIETY OF JAPAN, Vol. 93, No. 8, p. 587-595, August 1987

NUMERICAL SIMULATION OF THE UPLIFT OF THE TIBETAN PLATEAU

DAIGORO HAYASHI*

Abstract In order to simulate the formation of the Tibetan Plateau, several models are constructed assuming the crust as Newtonian fluid and the upper mantle lithosphere as rigid body. Calculations are performed for the period of 0.1 Ma after the collision because of the limitation of boundary conditions and the assumption of rigid lithosphere. Remarkable results are (1) emergence of Tibetan Plateau with 4000 m in height and (2) occurrence of great foredeep at the collided zone. With regard to the Himalayan nappe, the calculations which are continued during 1 Ma after the final stage of the collision obtain the following results : (1) viscous overturn movement around foredeep is probable to create the Himalayan nappe, (2) viscous flattening of the crust overcomes the upward movement of diapir.

Introduction

The "continent-continent collision" model for the uplift of Tibetan Plateau was recently treated quantitatively by ENGLAND and others (ENGLAND & MCKENZIE, 1982, 1983; ENGLAND & HOUSEMAN, 1985, 1986). These studies had assumed the Indian and Asian crusts to be incompressible non-Newtonian fluids and analyzed their collision in 3-dimension by means of a thin viscous sheet analysis with intention of explaining the structure of the interior of the Asian continent.

Even though their simulation may be one of the most reasonable collision models to take, it is impossible to elucidate the uplift of the Himalayas directly from their model. This is clear when we consider their model in Asia-India section. Their calculated results indicate always a vertical boundary truncated sharply along the middle of the Himalayan ranges and then India is not included in their analytical region (Fig. 1). Furthermore, they assume a perfect fluid lying underneath their thin viscous "Asia". However this boundary condition is not realistic as we know that the lithosphere beneath the continental crust differs considerably from a perfect fluid. The isostatic balance in their model is held at the expense of the artificial boundary setting.

In the present study, the uplift of the Tibetan Plateau and Himalayas is numerically simulated in due course of the northerly migration of the Indian plate deforming an incompressible Newtonian fluid of Asia above a rigid plate.

According to the rheological research of the crust and mantle, the upper crust behaves in a brittle manner and the lower crust obeys the law of Newtonian flow, while the mantle is governed by power law creep. On the contrary the lithosphere behaves like rigid body so far in the research of plate tectonics. This seems to be a discrepancy.

The present paper considers the upper mantle lithosphere as rigid body for the first approximation, and the deformable crust lies on the upper mantle. Then the deformation of the crust is expected to realize the plateau and mountain ranges. The idealized figure is shown as Fig. 2 from which we see that the isostatic readjustment is impossible and that the calculated values of the surface ascent are always overestimated compared to the reality. Furthermore, the rigid plate assumption prohibits the longer time simulation over 0.1 Ma.

Received February 24, 1987. Accepted June 22, 1987.

* Department of Marine Sciences, University of the Ryukyus, Nishihara, Okinawa, 903-01 Japan.

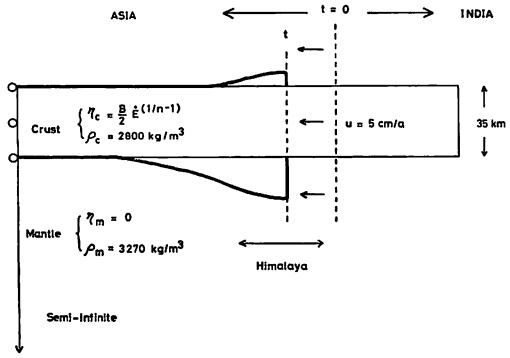

Fig. 1. Idealized boundary condition in 3-dimensional viscous thin sheet analysis after ENGLAND *et al.* (1982, 1983, 1985, 1986). B : depth-averaged strength coefficient, $\dot{E}$: second invariant of strain rate tensor, n : power law exponent, u : imposed boundary velocity, ρ_c : density of crust, ρ_m : density of mantle, η_c : viscosity coefficient of crust, η_m : viscosity coefficient of mantle.

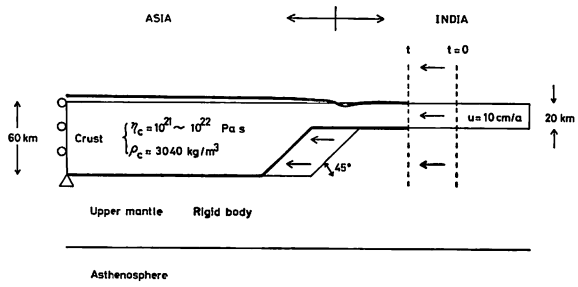

Fig. 2. Simplified boundary condition in the rigid plate model for models 9-1, 3, 5 in Fig. 4. This is not the case for models 13-1, 10-3, 11-1 in Fig. 4 where Indian plate stopped.

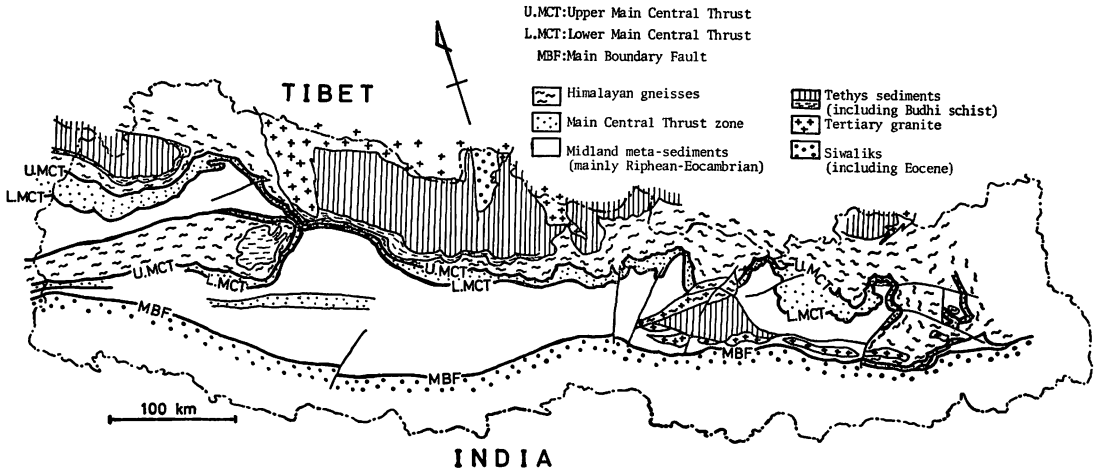

Fig. 3. Geological zonation of Nepal Himalayas (after ARITA, 1981, slightly modified).

With respect to the second theme, the cause of Himalayan nappe, we have enormous data from the field surveys (Fig. 3). Most important informations are summarized as follows.

The broad distribution of gneiss and schist formations on the Lesser Himalayan sequences signifies the extension on the south from the axial zone (the root zone) to MBF (Main Boundary Fault), as nappes of the "Himalayan gneiss zone thrust on the MCT (Main Central Thrust) zone". Generally, they show maximum thickness of 5 km and southern extension up to 100 km. Viewing by bird's eye, these nappes indicate extremely thin sheet layers compared to their broad distribution, and are composed of garnet biotite gneiss, calc-siliceous gneiss, augen gneiss and migmatitic gneiss, where the garnet biotite gneiss is

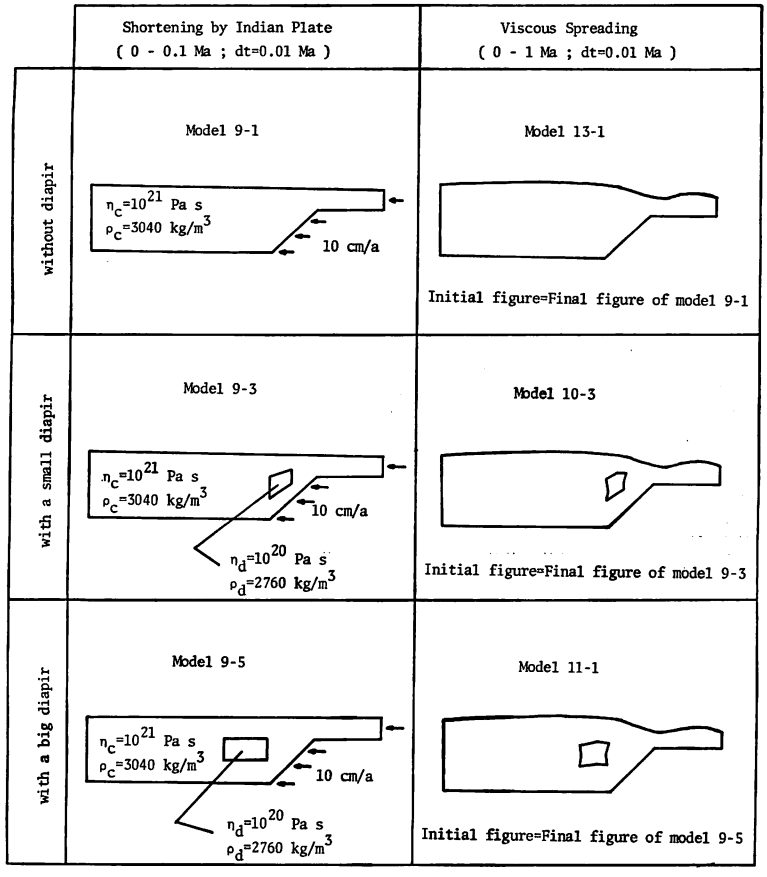

Fig. 4. Classification of models. dt : time interval of calculation, ρ_d : density of diapir, η_d : viscosity coefficient of diapir. Others are same as the explanation of Fig. 1.

dominated in general. This garnet biotite gneiss represents a banded structure of which the gneissosity is well developed. Although it is controversial whether the gneissosity shows the original bedding or not, the gneissosity is not disturbed in any way but stable. Therefore, it is a reasonable explanation that the nappes migrated about 100 km to the south along the MCT zone without disturbance.

Models

Models are divided into two groups.

(1) Shortening of the Asian crust by the Indian plate.

(2) Viscous spreading of the Asian crust after ceasing of compression by the Indian plate.

The model (1) is divided further into three subgroups.

(1.1) Shortening without diapir (Model 9–1).

(1.2) Shortening with a small diapir (Model 9–3).

(1.3) Shortening with a big diapir (Model 9–5).

The model (2) is also divided into three subgroups.

(2.1) Viscous spreading without diapir (Model 13–1).

(2.2) Viscous spreading with a small diapir (Model 10–3).

(2.3) Viscous spreading with a big diapir (Model 11–1).

The model (1) is established to simulate the collision of the Indian and Asian plates and to realize the Tibetan Plateau. Three models of (1) are different by means of the existence of diapir, and the size and place of diapir if it exists, with which we may recognize the effect of diapir in the event of plate collision.

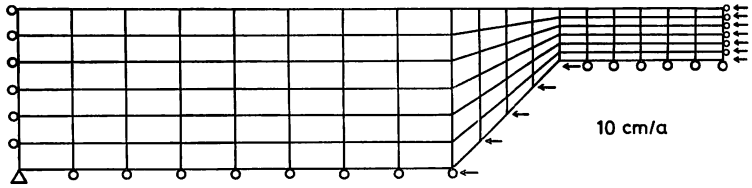

Fig. 5. Boundary condition and element partition of the model 9-1.

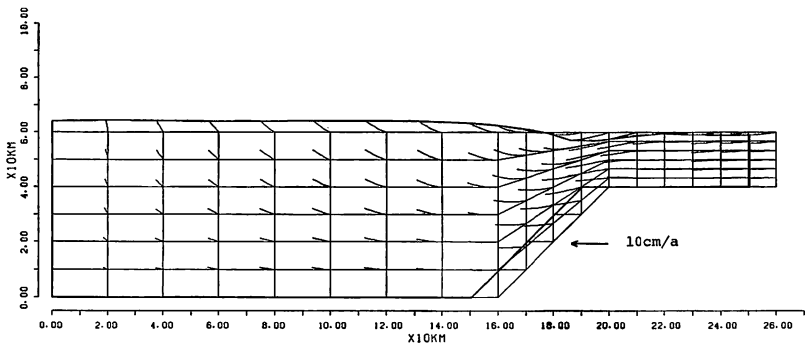

Fig. 6. Result of model 9-1. Solid line indicates the initial shape and trajectories of nodes, while bold line shows the final shape at 0.1 Ma.

However after 0.1 Ma which is rather small time scale for plate collision, it is impossible to continue to drive these shortening models any more under the assumption of rigid plate and the limitation of the analytical region.

In oder to simulate the collision of the Indian and Asian plates, the Indian crust of a 20 km thick is pushed against Asia of a 200 km long connected with a ramp inclined at 45 °. These boundary conditions are, however, taken without observational data.

Then, although it is unreasonable to consider the ceasing of migration of the Indian plate after 0.1 Ma, the author simulates the viscous rebound of the Asian crust after ceasing of the Indian plate movement, because it is valuable to see what the cause of nappe is and which movement is greater the upward migration of diapir or the viscous flattening movement of the crust. The simulations of the viscous spreading are performed during 1 Ma by the models 13–1, 10–3 and 11–1.

Conditions of all the models performed in the present paper are summarized in Fig. 4.

The numerical technique used for solving these models is based on the well known finite element method. When we want to treat with a Newtonian flow, we have to solve the governing equation of linear viscous flow.

$$v_{i,i}=0$$
$$-p_{,i}+\eta(v_{i,j})_{,j}+\rho f_i=0 \quad (i,j=1,2)$$

where x_i, v_i, p, η, ρ and f_i are Cartesian coordinate, velocity vector, pressure, shear viscosity, density and body force vector per unit mass, respectively. The derivative notation is defined as $v_{i,j}\equiv\partial v_i/\partial x_j$ and so forth. Since the corresponding fu nctional to th governing equation is known as,

$$\Pi[v_i,p]=\int_s\Big[\eta\Big\{v_{1,1}{}^2+\frac{1}{2}(v_{1,2}+v_{2,2})^2+v_{2,2}{}^2\Big\}-p(v_{1,1}+v_{2,2})-\rho(f_1v_1+f_2v_2)\Big]\,\mathrm{ds}$$

it is clear that the values of velocity and pressure for reasonable imposed boundary conditions can be obtained by the finite element technique.

The detailed formulation which derives a numerical scheme from the functional by means of the finite element method is given in HAYASHI (1979, 1984).

Shortening by the Indian plate

Shortening without diapir (Model 9–1)

Figure 5 illustrates boundary conditions and elements during the event of the collision of the Eurasian and Indian plates in Eocene. The area is divided into 108 isoparametric finite elements with 133 nodal points as il-

lustrated in the figure. As the maximum speed of the Indian plate is estimated to be 10 cm/a, the author takes this value as a boundary condition and assumes densities and viscosities of the Asian and Indian crusts as uniformly 3040 kg/m^3 and 10^{21} Pa·s respectively. Figure 6 shows that the Tibetan Plateau rises after 0.1 Ma about 4000 m and the surface of the Indian side subsides 1000—500 m from the original level where solid line draws the initial shape and grid, and the resultant shape indicated by bold line. Trajectory lines of each nodal point are shown by solid lines. It should be noted that there occurs a great foredeep of 3000 m in depth above the ramp. The relative rise of the Tibetan Plateau to India is about 4000 m or the relative amount from the bottom of the foredeep is about 7000 m.

The Tibetan Plateau extends 1000—1500 km to the north of the Himalayas. Therefore the analytical region would have to be taken greater than this model as shown in Fig. 7, however, in order to avoid the difficulty in the calculation only the region enclosed by the square is taken for analysis. If the analytical region is taken smaller than the real, the calculated value of uplifted amount is inevitably overestimated compared to the real value.

However, there is a relationship between calculated values and real uplifted values supposing that the viscosity of the crust is sufficiently small. Let consider Fig. 8 where the material of l in length and h in height is compressed laterally to result in the horizontal and vertical deformations a and b. The assumption of incompressibility provides the relation $b=ha/(1-a)$. As the real value of l is 1600 km and the set value of l in the model is 160 km, supposing b_{10} as the real risen value and b_1 as the calculated risen value, $b_1/b_{10}=\{-9/(a-1)\}+1$ is derived after simple manipulation. This curve realizes a hyperbola as illustrated in Fig. 9. Since the range of a dosen't exceed over 10 km, that is, 10 km/160 km=0.0625, we have $10 \leqq b_1/b_{10} \leqq 10.6$. Therefore, the real value of the uplift is estimated as about 1/10 of the calculated value.

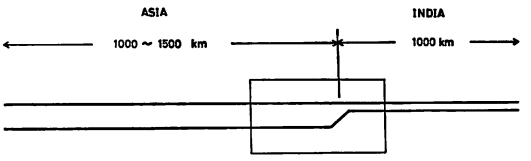

Fig. 7. Profile at collision of Asian and Indian plates. Area enclosed by square is the analytical region.

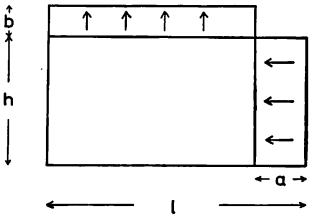

Fig. 8. Deformation of incompressible material (refer to text).

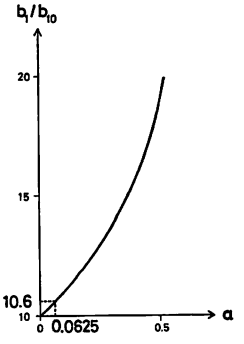

Fig. 9. Hyperbola of b_1/b_{10}-a diagram (refer to text).

Although it holds only after the undulation of surface is completely eliminated, it may be useful to infer the real values of the uplift from the calculated values.

Anyhow, the subject which the author intends to discuss, is whether there are uplifts on the Asian crust or not. The remarkable result is, the Tibetan Plateau with 4000 m height is realized after 1 Ma which is a deduced value by the above argument, but there are no tendencies of uplift among the collided area between both plates, whereas a great foredeep emerges.

From the trajectories of nodes in Fig. 6, it is clear that there is a critical area near the ramp where the directions of internal flow are changed. The flow within the Indian crust directs to north-downwards which causes

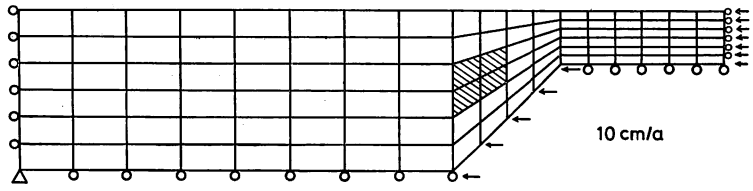

Fig. 10. Boundary condition and element partition of the model 9-3, where shaded area indicates diapir.

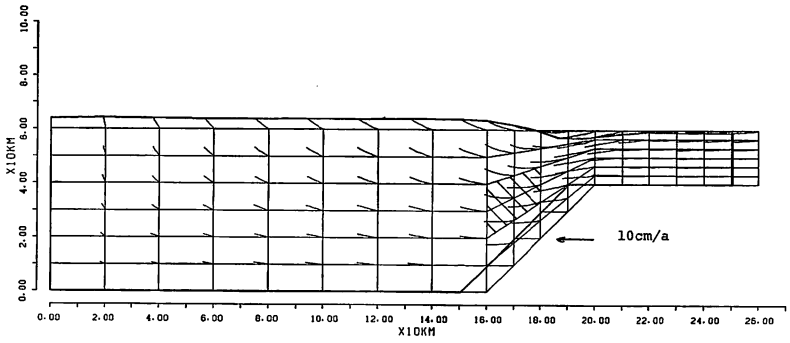

Fig. 11. Result of model 9-3. Others are same as the explanation of Fig. 6.

the great foredeep, on the contrary the flow within the Asian crust directs to north-upwards which involves the Tibetan Plateau.

Shortening with a small diapir (Model 9–3)

According to the data for the axial part of the Nepal Himalaya (GANSSER, 1964 ; HAGEN, 1969 ; HASHIMOTO *et al.*, 1973), so called the "root zone" produces a number of gneiss nappes or diapirs and granitic diapirs. The possibility to uprise the Himalayas resulted from diapirism is explored in this model.

The boundary conditions and the resultant figure are shown in Figs. 10 and 11 where a diapir is set up near the collided region. The density and viscosity of the diapir are 2760 kg/m^3 and 10^{20} Pa·s. This model results that the slope gradient of foredeep is slightly steeper and the surface just above the diapir rises slightly higher than the former model 9–1 (Fig. 6). There are no appreciable differences caused by a diapir among both figures.

Shortening with a big diapir (Model 9–5)

According to the idealized profile of the Nepal Himalaya (Fig. 12), many diapirs are situated under the Asian side. This fact is considered in this model.

The boundary conditions and the result are indicated in Figs. 13 and 14 where the greater diapir of 40×20 km is emplaced beneath the crust. The surface just above the diapir rises most among the models, about 5000 m above the original level or about 1000 m above the average level of the Asian surface, while the slope gradient of the foredeep is nearly the same as the model 9–1 (Fig. 6).

Viscous spreading

The possibility that the return flow within the Asian crust after the ceasing of plate movement is the cause of the Himalayan nappe will be examined during 1 Ma by the next models.

Viscous spreading without diapir (Model 13–1)

Initial boundary conditions are taken same as the final stage of model 9–1 (Fig. 6). Then the plates are stopped to move, in order to observe how the spreading of the crust goes on without the shortening by plate movement. The flattening process of the surface is going on as a result of the viscous flow of undulated surface. The result of the modelling will be used as a standard case of surface flattening. Even in the crust with a viscosity as 10^{21} Pa·s, the flattening is sufficiently soon to eliminate the foredeep after 1 Ma (Fig. 15).

We can recognize two regions of different property in the figure, the boundary of which

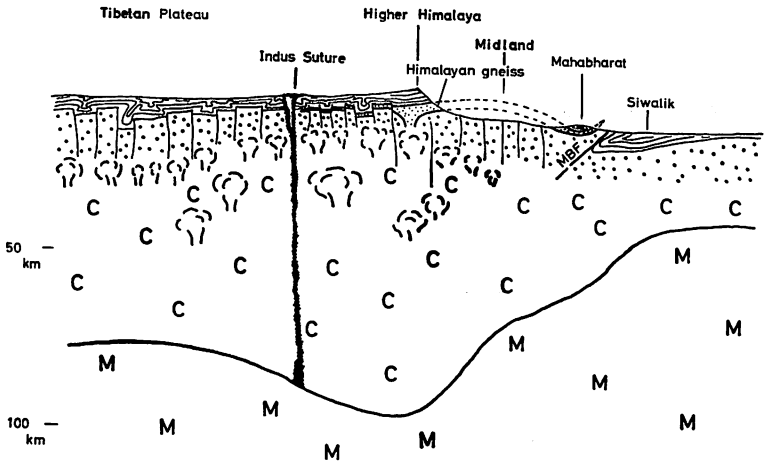

Fig. 12. Idealized profile of Nepal Himalayas. small spot : Himalayan gneiss, large spot : Precambrian to Paleozoic basement (Midland meta-sediments). C : lower crust. M : upper mantle (lower lithosphere), mushroom : diapir (after HAYASHI, 1980, slightly modified).

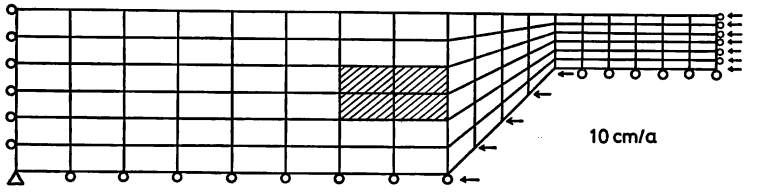

Fig. 13. Boundary condition and element partition of the model 9-5, where shaded area denotes diapir.

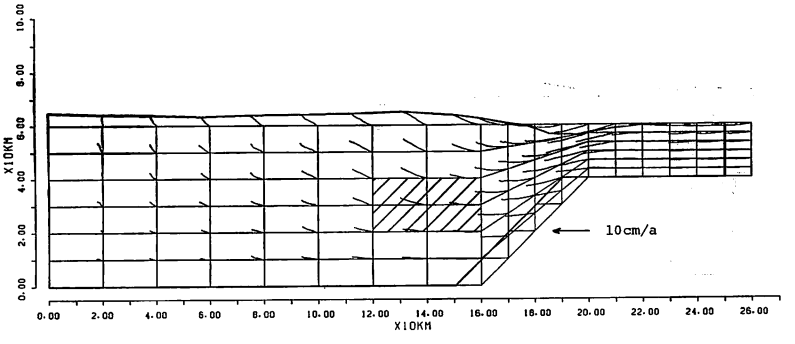

Fig. 14. Result of model 9-5. Others are same as the explanation of Fig. 6.

is placed near the intersect point of the initial and final ground surfaces (at about 150 km from northern edge). In the northern region the internal flow directs to south-downwards, while in the southern region south-upwards flow dominates. This south-upwards flow seems to be the cause of Himalayan nappe.

Viscous spreading with a small diapir (Model 10–3)

This model is the successor of the model 9–3. As indicated in Fig. 16, the surface uplift due to diapir upwelling is cancelled by the viscous flow of the crust, and the height of the surface even above the diapir of after 1 Ma is only 500 m. The remarkable difference from the model 13–1 is that the internal flow around and within the diapir directs upwards steeper than the model 13–1.

Viscous spreading with a big diapir (Model 11–1)

This is the successor of the model 9–5. As shown in Fig. 17, both levels of the surfaces just above the diapir and of the Indian side rise mildly around 1000—2000 m than the average level of the Asian side surface, however, it may not be expected to rise due to the

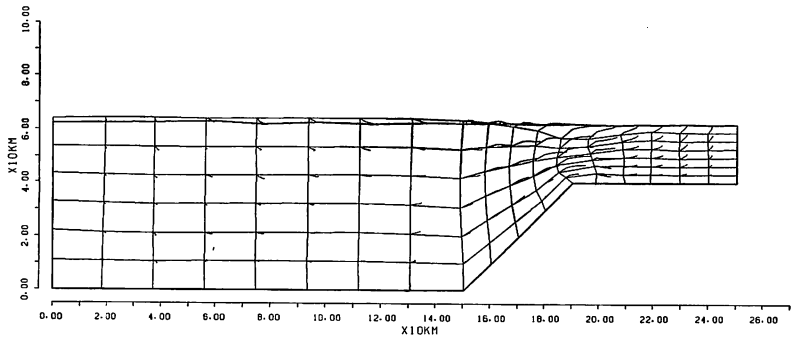

Fig. 15. Result of model 13-1. Solid line indicates initial shape (final shape of the model 9-1 at 0.1 Ma) and trajectories of nodes. Bold line denotes final shape at 1 Ma after ceasing of the Indian plate.

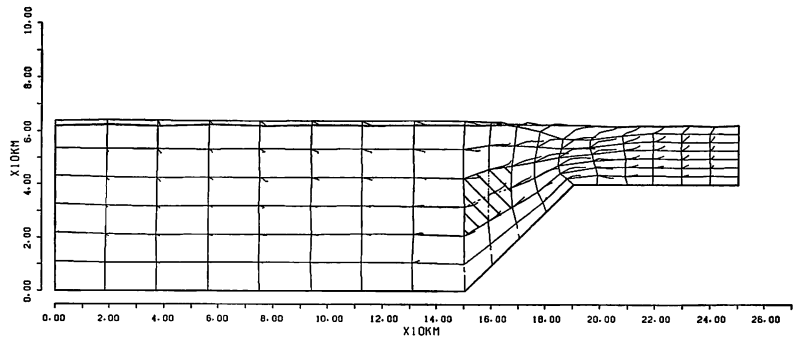

Fig. 16. Result of model 10-3. Solid line indicates initial shape (final shape of the model 9-3 at 0.1 Ma) and trajectories of nodes. Others are same as the explanation of Fig. 15.

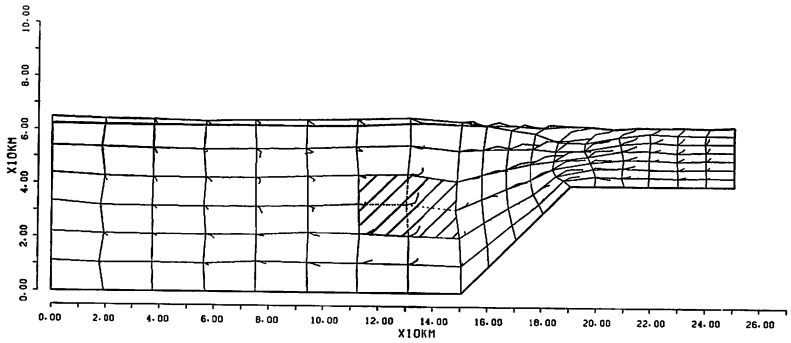

Fig. 17. Result of model 11-1. Solid line indicates initial shape (final shape of the model 9-5 at 0.1 Ma) and trajectories of nodes. Others are same as the explanation of Fig. 15.

diapir upwelling any more. The internal flow near the diapir directs incredibly steeper and more complex than the models 13–1 and 10–3.

Conclusions

Results obtained from the simulation are summarized as follows.

(1) Tibetan Plateau with 4000 m in height emerged after 1 Ma (deduced value) from the collision of the Asian and Indian plates where the relative speed of the Indian plate is 10 cm/a.

(2) Great foredeep with 3000 m in depth occurs after 1 Ma (deduced value) resulted from the collision of both plates. It is suggestive to consider the cause of the Siwalik basin but is problematic because of too early emergence.

(3) Himalayan nappe is very likely to be introduced by the return flow of the Asian crust after the ceasing of both plate movements.

(4) Viscous flattening of the crust is sufficiently strong to overcome the mountain building movement due to diapirism.

However, there are following many problems

in the conditions of the simulation:

(1) Rigid plate assumption.
(2) Too narrow analytical region (260 km long).
(3) Too fast plate movement (10 cm/a).
(4) 45 °-inclined ramp which is not based on the field observations.
(5) Setting of too thick initial Asian crust (60 km) compared to the Indian crust (20 km), the setting of which is forced by the rigid plate assumption.

These defects are necessary to be removed in the future simulation.

Acknowledgements

The author should like to acknowledge to Prof. em. Hans RAMBERG and Prof. Christopher TALBOT of University of Uppsala and Prof. Koshiro KIZAKI of University of the Ryukyus for their help during the study.

References

ARITA, K., 1981 : Geology of the Himalayas, with special reference to the Nepal Himalayas. *Recent Progress of Natural Sciences in Japan*, 6, 76–83.

ENGLAND, P. and HOUSEMAN, G., 1985 : Role of lithospheric strength heterogeneities in the tectonics of Tibet and neighbouring regions. *Nature*, **315**, 297–301.

———— and ————, 1986 : Finite strain calculations of continental deformation. 2. Comparison with the India-Asia collision zone. *J. Geophys. Res.*, **91**, 3664–3676.

———— and MCKENZIE, D., 1982 : A thin viscous sheet model for continental deformation. *Geophys. J. R. astr. Soc.*, **70**, 295–321.

———— and ————, 1983 : Correction to : a thin viscous sheet model for continental deformation. *Ibid.*, **73**, 523–532.

GANSSER, A., 1964 : *Geology of the Himalayas*. 289p., John Wiley and Sons Ltd.

HAGEN, T., 1969 : Report on the geological survey of Nepal, vol. 1, *Denkschr. Schweiz. Naturf. Gesell.*, **86**, 185 p.

HASHIMOTO, S., OHTA, Y. and AKIBA, C. (eds.), 1973 : *Geology of the Nepal Himalayas*. 292p., Saikon.

HAYASHI, D., 1979 : Finite element formulation of viscous fluid based on a variational principle. *Bull. Coll. Sci., Univ. Ryukyu*, no. 28, 119–130.

————, 1980 : Simulation of Himalayan orogeny and tectonophysics. *Monthly Earth*, **2**, 787–796.*

————, 1984 : Dynamics of plutonism. *Ibid.*, **6**, 290–298.*

* : in Japanese

(要　旨)

HAYASHI, D., 1987 : Numerical simulation of the uplift of the Tibetan Plateau. *Jour. Geol. Soc. Japan*, 93, 587-595. (林大五郎, 1987：チベット高原隆起の数値シミュレーション. 地質雑, **93**, 587-595)

チベット高原の形成をユーラシアプレートおよびインドプレートの衝突によって説明するために，地殻を Newton 流体と，またリソスフェアを剛体と見なして数値シミュレーションを行った．境界条件の制約から衝突後の 0.1 Ma(10 万年) 間を計算した．主な結果として（1）4000 m に達するチベット高原の出現（2）衝突部の大規模な前縁凹地，を得た．

ヒマラヤ・ナップの原因について，上記の衝突後のモデルを初期境界条件として 1 Ma(100万年) 間にわたる数値シミュレーションを行った．結果として（1）前縁凹地周辺の粘性逆転運動がヒマラヤ・ナップを形成した，（2）地殻の粘性流動による平坦化がダイアピル上昇を凌駕する，を得た．